https://doi.org/10.5194/egusphere-2023-1496
Preprint. Discussion started: 14 July 2023

Resolving the mesoscale at reduced computational cost with FESOM 2.5: efficient modeling approaches applied to the Southern Ocean

Nathan Beech[1], Thomas Rackow[2], Tido Semmler[3], and Thomas Jung[1,4]

1. Alfred Wegener Institute Helmholtz Center for Polar and Marine Research, Bremerhaven, Germany

2. European Center for Medium-range Weather Forecasts, Bonn, Germany

3. Met Eireann, the Irish Meteorological Service, Dublin, Ireland

4. Department of Physics and Electrical Engineering, University of Bremen, Bremen, Germany

Corresponding Author: Nathan Beech (Nathan.beech@awi.de)

https://doi.org/10.5194/egusphere-2023-1496
Preprint. Discussion started: 14 July 2023

Abstract

Several cost-efficient, high-resolution modeling approaches are applied to simulations of the Southern Ocean in past, present, and future climates. The results are compared with an ensemble of medium-resolution, eddy-present simulations and evaluated based on their ability to reproduce observed mesoscale activity and to reveal a response to climate change distinct from natural variability. The high-resolution simulations reproduce the observed magnitude of Southern Ocean eddy kinetic energy (EKE) well, but differences remain in local magnitudes and the spatial distribution of EKE. The coarser, eddy-present ensemble simulates a similar pattern of EKE but underrepresents observed levels by 50%. Five years of simulated data in each time period is found to produce consistent results when evaluating mean conditions and assessing change in the region as a whole. At 1 °C of warming, the high-resolution simulations produce no change in overall EKE, in contrast to the increase projected by the eddy-permitting ensemble and despite full ensemble agreement. At 4 °C of warming, both datasets produce consistent levels of EKE rise in relative terms, although not absolute magnitudes, as well as an increase in EKE variability. Simulated EKE rise is concentrated where flow interacts with topographic features in regions already known to be eddy-rich. Regional EKE change in the high-resolution simulations is consistent with changes seen in at least four of five eddy-permitting ensemble members at 1 °C of warming, and all ensemble members at 4 °C. However, substantial noise would make these changes difficult to distinguish from natural variability without an ensemble.

Plain Language Summary

Ocean models struggle to simulate small-scale ocean flows due to the computational cost of high-resolution simulations. Several cost-reducing strategies are applied to simulations of the Southern Ocean and evaluated with respect to observations and traditional, lower-resolution modelling methods. The high-resolution simulations effectively reproduce small-scale flows seen in satellite data and are largely consistent with traditional model simulations regarding their response to climate change.

https://doi.org/10.5194/egusphere-2023-1496
Preprint. Discussion started: 14 July 2023

1 Introduction

Mesoscale activity in the Southern Ocean has been the subject of much research and interest in recent years due to the intensification of Southern Hemisphere westerlies (Marshall, 2003), the phenomena of eddy saturation and compensation (Munday et al., 2013; Bishop et al., 2016), and the potential for carbon sequestration in the face of ongoing anthropogenic emissions (Sallée et al., 2012; Landschützer et al., 2015; Frölicher et al., 2015). Observations already reveal an intensification of eddy activity in the Antarctic Circumpolar Current (ACC) and changes are attributed primarily to wind stress (Marshall, 2003; Hogg et al., 2015; Martínez-Moreno et al., 2021). Modeling studies have been able to reproduce the observed changes, as well as project continued intensification throughout the 21st century (Beech et al., 2022), but the modeled results rely on only partially resolved eddy activity relative to observations, leaving open the possibility for new findings or greater clarity.

Advances in computational capabilities have enabled ocean modeling science to make great progress in overcoming the substantial computational burden of simulating the mesoscale, but shortcomings remain, particularly in the Southern Ocean where the Rossby radius can be as small as 1 km, increasing the computational cost of resolving eddies (Hallberg, 2013). Even model resolutions that can generally be considered eddy-resolving are only eddy-permitting poleward of 50° if they do not vary in space (Hewitt et al., 2020). This highlights an efficiency challenge in simulating the mesoscale with traditional model grids; resolutions necessary to resolve high-latitude, small-radius eddies are both prohibitively expensive and unnecessary to resolve mesoscale eddies in the lower latitudes. Fortunately, a growing number of modelling alternatives to traditional grids now enable dynamic spatial allocation of resources (Danilov, 2013; Ringler et al., 2013; Danilov et al., 2017; Jungclaus et al., 2022), creating the opportunity to more efficiently resolve the mesoscale.

As resource allocation in high-resolution modeling becomes spatially flexible in the pursuit of more efficient configurations, the temporal component must also be scrutinized for efficiency. Traditional modeling approaches require long spin-up periods in order to equilibrate the deep ocean and reduce model drift (Irving et al., 2021). Although the impacts of drift are not negligible, it generally affects large-scale processes in the deep ocean; mesoscale processes that require high resolutions to simulate are typically fast-to-equilibrate and will appear relatively quickly wherever large-scale ocean conditions lead to their creation. Admittedly, one cannot entirely disentangle the two scales, as mesoscale activity does affect the position of fronts and the paths of ocean circulation (Marzocchi et al., 2015; Chassignet and Xu, 2017). Yet, with equilibration times for the deep ocean on the scale of thousands of years (Irving et al., 2021), the possibility, and ultimately necessity, to reduce the resolution of spin-up runs relative to production runs must be investigated.

Advancing the concept of dynamic temporal allocation of resources further, the traditional transient climate change simulation also represents an efficiency bottleneck for some applications; by modifying the climate continuously in time, each year of a transient simulation is effectively a single realization of a global mean climatic state that varies from the following and preceding years by only a fraction of a degree. For some applications, like hindcasts of real events or trend analysis, this approach may be desirable, but for assessing the impacts of climate change with limited resources and a low signal-to-noise ratio, a larger sample of realizations for a consistent climatic state may be more suitable.

Aside from oceanic concerns, the atmosphere can have substantial impacts on mesoscale activity in climate models. Most simply, a coupled atmosphere will react to ocean eddy activity, whereas atmospheric forcing will not, resulting in more eddy killing by wind stress (Renault et al., 2016). Additionally, an atmosphere coupled to a high-resolution ocean must be of similarly high resolution for certain mesoscale interactions to be resolved (Byrne et al., 2016). Ultimately, the modeled atmosphere further escalates the already exponential cost of increasing ocean resolution by requiring more computational resources in order for the benefits of the resolved mesoscale to fully transfer to the broader climate.

To address the computational inefficiencies outlined above, an experimental configuration is proposed, combining several experimental modeling approaches. Simulations will exploit the multi-

https://doi.org/10.5194/egusphere-2023-1496
Preprint. Discussion started: 14 July 2023

resolution Finite volumE Sea-ice Ocean Model (FESOM) (Danilov et al., 2017) employing a high-resolution unstructured mesh that concentrates computational resources on the Southern Ocean, while maintaining grid resolution in the remainder of the global ocean that can still be considered high-resolution, as in, for example, HighResMIP (Haarsma et al., 2016). The multi-resolution strategy overcomes the efficiency challenges of resolving high-latitude eddies without needlessly increasing tropical resolutions, as well as limiting the focus and computational requirements to one hemisphere. The high-resolution simulations will make use of a spin-up simulation on a medium-resolution, eddy-permitting mesh to avoid the computational burden of allowing an eddy-resolving ocean to equilibrate deep, slow-changing processes. The eddy-permitting mesh will also be used to simulate the transient periods between shorter, high-resolution time slices, increasing the signal-to-noise ratio of the results by separating the production data further in time and the progression of anthropogenic climate change. Finally, the ocean model will be forced with atmospheric data from existing coupled simulations (Semmler et al., 2020). Although this will not facilitate mesoscale atmosphere-ocean interaction, the simulation will reflect the climatic development of an eddy-permitting simulation of the future atmosphere without the additional computational requirements.

The Southern Ocean is one of the world's hotspots for mesoscale activity and a region where substantial change is anticipated in the context of anthropogenic climate change (Beech et al., 2022). Simultaneously, the high latitude of the region makes eddy-resolving model simulations computationally demanding and observational data relatively scarce (Auger et al., 2023; Hallberg, 2013). Yet, as the climate changes, the importance of the Southern Ocean grows as a heat and carbon sink, an ecosystem, and a medium for feedback between the atmosphere and ocean (Byrne et al., 2016; Frölicher et al., 2015). Thus, the study of the Southern Ocean demands innovation in the modeling field to produce high-resolution simulations at reduced computational cost. This study maximizes grid resolution relative to computational cost using an unstructured, multi-resolution grid, a medium-resolution spin-up simulation, and atmospheric forcing from lower-resolution coupled simulations in order to focus resources as much as

https://doi.org/10.5194/egusphere-2023-1496
Preprint. Discussion started: 14 July 2023

possible on resolving mesoscale activity in the study region. The resulting simulations enable an exploratory analysis of the past, present, and future of the Southern Ocean with a fully resolved mesoscale. Simulations with this cost-efficient, high-resolution configuration are presented in comparison to a comprehensive ensemble of eddy-permitting simulations to assess the performance of the efficiency-focused approach in reproducing mesoscale activity and its response to climate change.

2 Methods

2.1 Experimental setup

This analysis is broadly a comparison of results from AWI-CM-1-1-MR's contribution to CMIP6 (hereafter referred to as AWI-CM-1) (Semmler et al., 2020) and simulations using an updated version of FESOM (FESOM 2.5) and a mesh substantially refined to a resolution reaching less than 3 km in the Southern Ocean (hereafter referred to as SO3) (Supplementary Figure 1). Observations of ocean surface velocity derived from satellite altimetry data are also used to evaluate the model performance of each simulation. The AWI-CM-1 simulations are state-of-the-art CMIP6 experiments and benefit from the multiple ensemble members and long spin-up times that CMIP simulations typically boast. However, while the AWI-CM-1 ensemble reproduces eddy activity remarkably well within the context of CMIP6 (Beech et al., 2022), high-resolution ocean modeling now far surpasses even the highest ocean resolutions in the CMIP6 ensemble. Conversely, the SO3 simulations push the limits of ocean resolution but rely on several measures for maximizing computational efficiency that may impact the robustness of the simulations. Details on the experimental setup for CMIP6 and ScenarioMIP are widely available (Eyring et al., 2016; O'Neill et al., 2016) and information more specific to AWI-CM-1-1-MR's contribution has been published previously (Semmler et al., 2020). The following sections will outline the details of the SO3 simulations.

The model experiments with SO3 consist of a medium-resolution, eddy-permitting, ocean-only transient simulation from 1851-2100 and three shorter simulations with the SO3 mesh at different time

https://doi.org/10.5194/egusphere-2023-1496
Preprint. Discussion started: 14 July 2023

periods during the progression of anthropogenic climate change. The medium-resolution transient run is a stand-alone ocean simulation using a medium-resolution mesh that has been shown to effectively reproduce eddy activity in active regions while maintaining a computational cost comparable to a traditional ¼ ° model (Beech et al., 2022). The model is initialized with conditions for ocean temperature and salinity, as well as sea ice concentration, thickness, and snow cover taken from the end of the first year (1850) and first ensemble member (r1i1p1f1) of AWI-CM-1-1-MR's historical simulations in CMIP6 (Semmler et al., 2018, 2020, 2022a, b). In this way, the model undergoes a semi-cold start in which ocean conditions are not exact continuations of the previous coupled simulation, but nonetheless benefit from more realistic and partially equilibrated ocean properties. The stand-alone ocean is forced using atmospheric data from the same ensemble member of the historical CMIP6 simulations until 2014 (Semmler et al., 2022a), and thereafter using the first ensemble member of AWI-CM-1-1-MR's ScenarioMIP simulations for shared socioeconomic pathway (SSP) 3-7.0 (Eyring et al., 2016; O'Neill et al., 2017; Semmler et al., 2022b). This approach to forcing takes advantage of a coupled simulation, CMIP6, to produce a forcing dataset of better temporal and spatial coverage than the observational record and which maintains a realistic transient climate throughout anthropogenic impacts during the 21st century.

In the years 1950, 2015, and 2090, the model is reinitialized with the higher-resolution ocean grid, SO3 (Supplementary Figure 1), using the same semi-cold start approach and forcing dataset, as well as initial conditions from the end of the previous year of the eddy-permitting transient simulation. The high-resolution grid is, in truth, a regionally refined mesh in which a 25 km global resolution is increased to approximately 2.5 km primarily south of 40 °S, but with other pertinent regions, such as the Agulhas Current and several narrow straits, also refined. In this way, the model is able to simultaneously achieve eddy-rich conditions in the Southern Ocean and many of the nearby active regions as well as a global resolution that would still be considered high in the context of CMIP6 (Hallberg, 2013; Hewitt et al., 2020). The high-resolution simulations are each integrated for six years with the first year ignored as a

https://doi.org/10.5194/egusphere-2023-1496
Preprint. Discussion started: 14 July 2023

true spin-up, leaving five years of data for each time period. While model drift may be a concern with such a short true spin-up period, this should affect each of the high-resolution time slices similarly and to a limited extent due to their short integration lengths. Thus, the differences between the high-resolution ocean simulations should primarily reflect anthropogenic climate impacts simulated during the eddy-permitting transient run.

2.2 Model configuration

The Finite volume Sea-ice Ocean Model version 2.5 is a post-CMIP6 era model, having been refactored to a finite-volume configuration from the finite-element version (FESOM1.4, Q. Wang et al., 2014) employed in CMIP6, and transitioned to arbitrary Lagrangian Eulerian (ALE) vertical coordinates, among other improvements (Danilov et al., 2017; Scholz et al., 2019, 2021). FESOM's most distinguishing feature among mature ocean models is the unstructured horizontal grid that exploits triangular grid cells which can smoothly vary in size to change the horizontal grid resolution in space. In these simulations, full free surface, or z*, vertical coordinates were used, allowing the vertical model layer thicknesses to change in time. Gent-McWilliams eddy parameterization (Gent and McWilliams, 1990) is scaled with resolution according to (Ferrari et al., 2010) and vertical mixing is simulated by a *k*-profile parameterization scheme (Large et al., 1994).

The SO3 mesh consists of over 22 million surface elements (triangle faces) or 11 million surface nodes (triangle vertices) and 70 vertical layers. The simulations produce about 1.1 terabytes of data per year of 3D data stored on nodes. The model was run on 8192 CPU cores and with a typical throughput of approximately 0.65 simulated years per day, consuming approximately 5.5 million CPU hours in total despite the various cost-saving modeling approaches. The simulations and following analysis were performed using the high-performance computing system, Levante, at the German Climate Research Center (DKRZ).

https://doi.org/10.5194/egusphere-2023-1496
Preprint. Discussion started: 14 July 2023

The ocean model is forced by several atmospheric variables at a six-hour resolution, although one forcing variable, humidity, is interpolated monthly data. The forcing data is first interpolated to a regular grid which can be interpreted by the model and applied to the multi-resolution grid used in the respective simulations. Runoff data is a monthly climatology and dynamic ice sheet coupling is not included, meaning the freshwater influx from the Antarctic continent does not react to warming which may impact certain processes, such as the timing and intensity of sea ice loss (Pauling et al., 2017; Bronselaer et al., 2018).

2.3 Altimetry data

Daily geostrophic velocities are taken from a gridded altimetry product derived from crossover data available from the Data Unification and Altimeter Combination System (DUACS) (Taburet et al., 2019). The gridded product has a resolution of 0.25 °, although effective resolution at high latitudes may be much lower (Ballarotta et al., 2019). Recently, improved data has become available in the ice-covered regions of the Southern Ocean (Auger et al., 2022), but does not yet cover the present-day simulated period (2016-2020) in this study. Absolute velocities from the gridded altimetry product were used to calculate anomalies and EKE using equations (3) and (4) below for consistency with the modeled dataset.

2.4 Geostrophic velocities

Ocean velocities in the SO3 simulations are saved on a daily timescale as direct model output, whereas in the AWI-CM-1 ensemble, only monthly data is available and daily data must first be derived from sea surface height data and geostrophic balance as in equations (1) and (2). To avoid including ageostrophic contributions to ocean surface velocity in this analysis, model output velocity between 25 m and 30 m depth is used for the SO3 dataset. This depth should be close enough to the surface to closely match surface geostrophic flows while also avoiding Ekman transport, a major contributor to ageostrophic ocean flow. What ageostrophic flow remains in the model output velocities should be primarily large-

https://doi.org/10.5194/egusphere-2023-1496
Preprint. Discussion started: 14 July 2023

scale and overshadowed by geostrophic flow in the high-energy regions of the ocean, including the ACC (Yu et al., 2021).

$$u = -gf^{*}\partial SSH/\partial y \qquad (1)$$

$$v = gf^{*}\partial SSH/\partial x \qquad (2)$$

e. EKE analysis

Velocity anomalies are defined by subtracting the multi-year monthly climatology of each respective 5-year period from daily velocities with equation (3).

$$u'_i = u_i - \overline{u_m} \qquad (3)$$

Where u_i is the daily zonal velocity, ‘ denotes an anomaly, and $\overline{u_m}$ is a monthly mean. For meridional velocities (v) substitute u with v.

Eddy kinetic energy is calculated from ocean velocities according to equation (4).

$$EKE_i = 0.5({u'_i}^2 + {v'_i}^2) \qquad (4)$$

Where ($_i$) denotes a daily value and (‘) denotes an anomaly.

EKE was calculated on the native grid of each dataset and then interpolated to a 0.25 ° grid for all analyses. EKE in Figures 1 and 3 was coarsened to five-day means before analysis. Area-integrated EKE is calculated by summing the area-weighted EKE of each grid cell in the study region defined as the zonal band between 45 °S and 60 °S with the Brazil/Malvinas confluence region between 57 °E and 29 °E and northward of 40 °S removed. EKE anomalies (Figure 1) were calculated by subtracting the 2016-2020 mean from the EKE data of each period. Normalized EKE was calculated by further dividing EKE anomaly by the standard deviation of EKE during the 2016-2020 period. In Figure 4, ensemble agreement is determined by ordering the ΔEKE values within each grid cell from lowest to highest, plotting the

https://doi.org/10.5194/egusphere-2023-1496
Preprint. Discussion started: 14 July 2023

positive values in increasing order from left to right and negative values in decreasing order from left to right.

3 Results

3.1 Agreement with observations

During the five-year period of overlap with observations, the SO3 simulation is a drastic improvement on the AWI-CM-1 ensemble in reproducing median observed EKE (Figure 1a, c); only a slight underrepresentation of EKE remains in the SO3 simulation, although the simulated distribution remains distinct from observations, whereas the AWI-CM-1 ensemble underrepresents observations by about 50% (Figure 1a, c). EKE in SO3 appears more variable than the observations as can be inferred from the larger range (Figure 1c, e) and its distribution appears less Gaussian than observations or the eddy-permitting dataset (Figure 1a, b, c). Taking the AWI-CM-1 ensemble as an example, there is no consistent pattern of multimodality or skewness and the ensemble mean more closely approximates the normal distribution than the individual members (Figure 3), suggesting that deviations from normality could be primarily due to sample size rather than the character of the data. Relative to the AWI-CM-1 model bias and the magnitude of EKE resolved, the ensemble spread within the AWI-CM-1 dataset is small (Figure 3), suggesting that a single ensemble member of five years duration is sufficient to assess how well a model captures the overall magnitude of Southern Ocean EKE (Figure 1c).

https://doi.org/10.5194/egusphere-2023-1496
Preprint. Discussion started: 14 July 2023

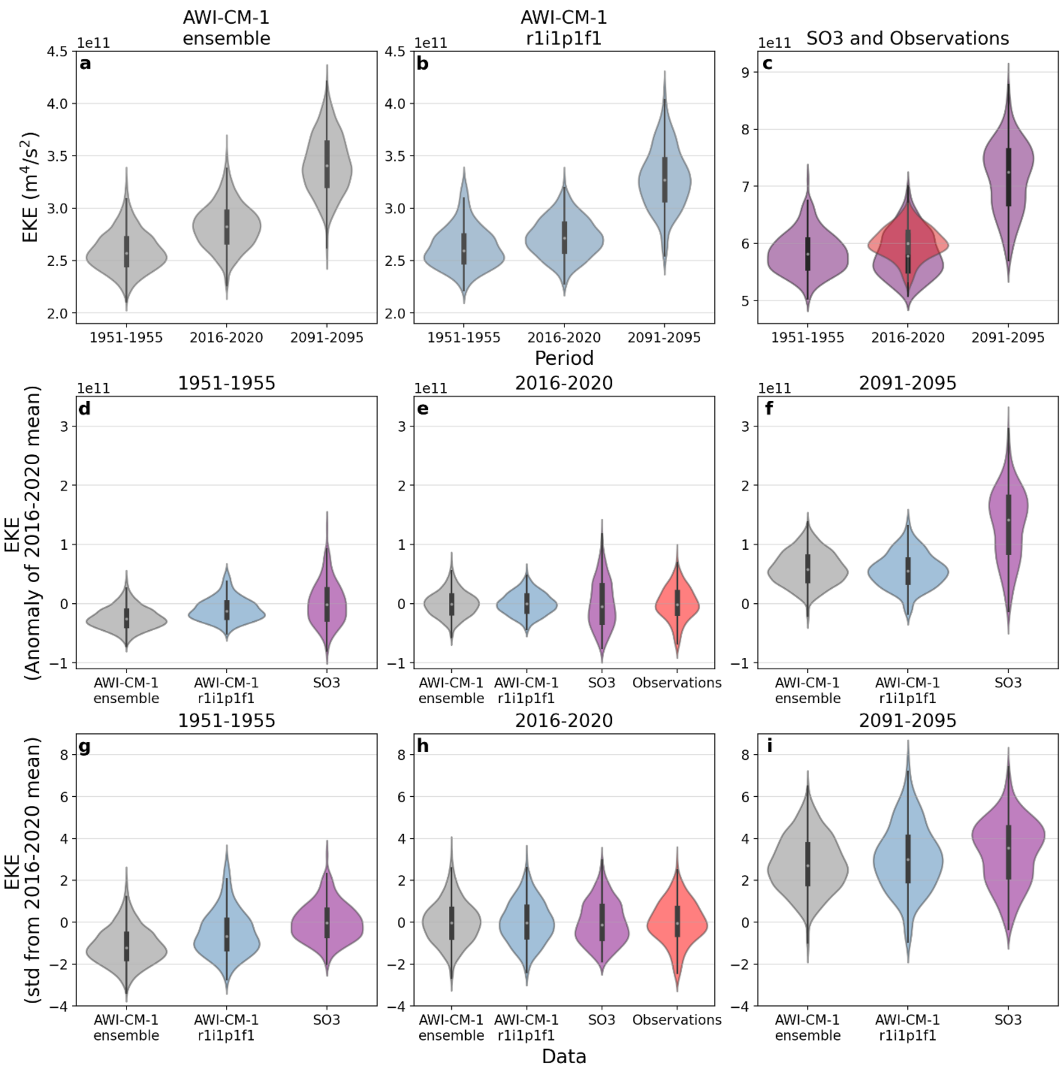

Figure 1. Violin plots of EKE in simulations and observations. Central points of each plot indicate the median, thick bars span the first and third quartiles, thin bars span the range, and the violin body is a kernel density estimation of the data. **a-c)** Real magnitudes of EKE (note the different y axes) **a)** The AWI-CM-1 ensemble. **b)** the first member of the AWI-CM-1 ensemble, from which the SO3 simulations take their atmospheric forcing. **c)** The So3 simulations and observations. **d-f)** EKE anomalies relative to the 2016-2020 mean for each dataset respectively. **d)** 1951-1955. **e)** 2016-2020. **f)** 2091-2095. **g-i)**

https://doi.org/10.5194/egusphere-2023-1496
Preprint. Discussion started: 14 July 2023

Normalized values relative to the mean and standard deviation of EKE during the 2016-2020 period for each dataset respectively. **g)** 1951-1955. **h)** 2016-2020. **i)** 2091-2095.

From a regional perspective, the SO3 simulation accurately reflects local magnitudes of observed EKE and also generally captures the spatial distribution well (Figure 2). However, there are regional shortcomings, such as between 90 and 145 °E. Grid resolution in this region should be sufficient to resolve eddy activity (Supplementary Figure 1), indicating that the bias arises from another source. In the AWI-CM-1 ensemble, the regional representation of EKE reinforces a broad underrepresentation relative to observed magnitudes, but the major geographic features of eddy activity are fairly well represented (Figure 2). Once again, the ensemble spread within the AWI-CM-1 simulations reveals remarkable consistency, this time in terms of the spatial pattern and regional magnitudes (Supplementary Figure 2), reinforcing the conclusion that a single ensemble member of five years duration is sufficient to assess the mean state of EKE in the Southern Ocean. The consistency of the AWI-CM-1 ensemble further suggests that regional shortcomings in eddy activity in the SO3 simulations are not a product of variability within a single realization of Southern Ocean conditions (Supplementary Figure 2).

https://doi.org/10.5194/egusphere-2023-1496
Preprint. Discussion started: 14 July 2023

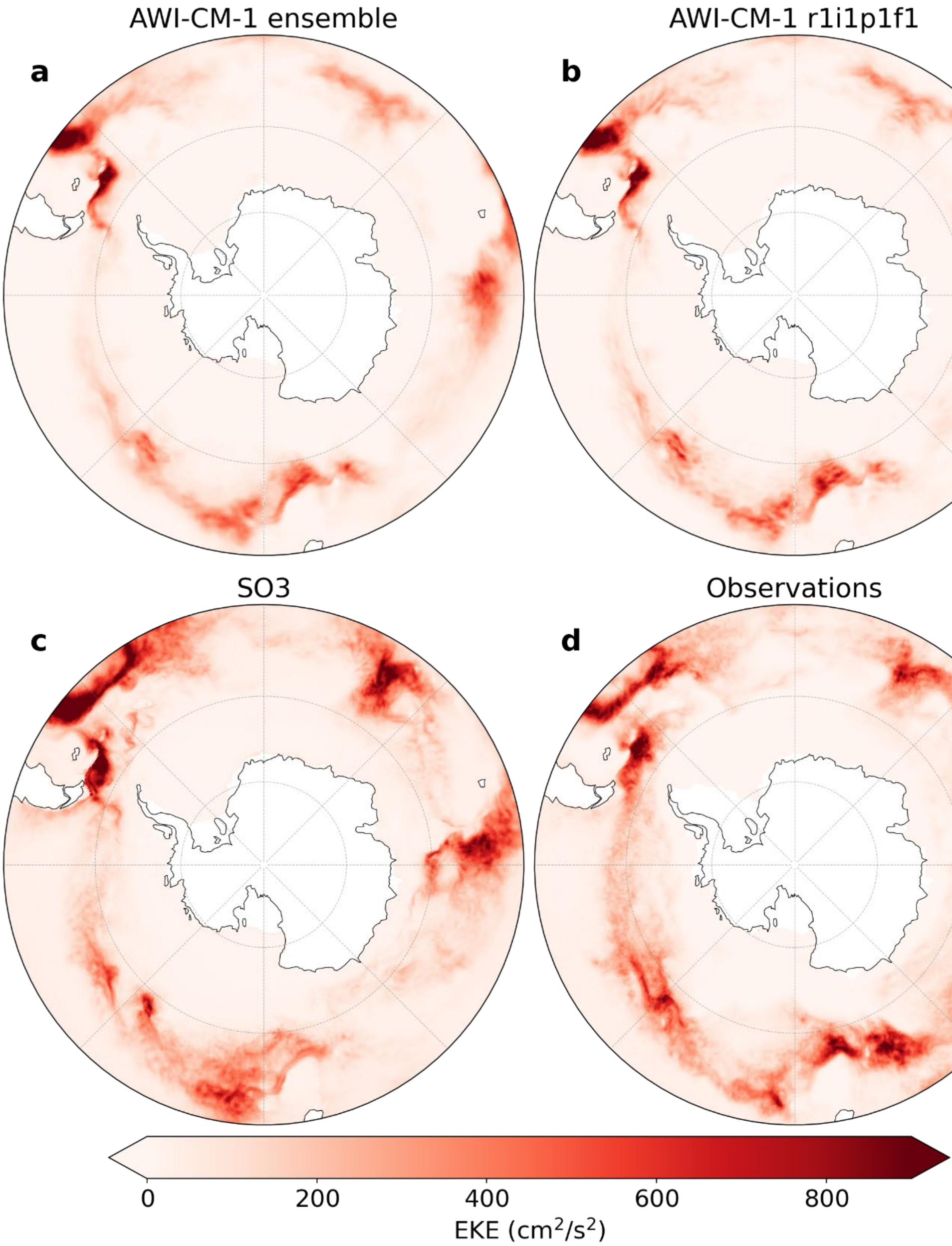

Figure 2. Mean eddy kinetic energy between 2016 and 2020. a) The AWI-CM-1 ensemble. **b) T**he first member of the AWI-CM-1 ensemble. **c)** The SO3 simulation. **d)** The gridded satellite altimetry dataset.

https://doi.org/10.5194/egusphere-2023-1496
Preprint. Discussion started: 14 July 2023

3.2 EKE change and significance

Southern Ocean eddy activity has been shown to intensify over the recent decades both using satellite altimetry (Martínez-Moreno et al., 2021), and the complete AWI-CM-1 dataset from CMIP6 (Beech et al., 2022). Even after reducing the AWI-CM-1 CMIP6 dataset to five-year periods preceding the apparent change (1951-1955) and at the end of the altimetry era (2016-2020), this intensification is still discernable within the AWI-CM-1 ensemble (Figure 1a). Despite this, the SO3 simulations do not demonstrate any substantial change in magnitude over the same period (Figure 1). Further reducing the ensemble to its individual members, the EKE rise is still relatively clear in each case considering the median, mode, and first and third quartiles of the distributions (Figure 3), suggesting again, that natural or internal variability is not responsible for the discrepancies between simulations. Therefore, despite the first AWI-CM-1 ensemble member, from which the SO3 simulations receive their atmospheric forcing, producing lower-than-average EKE rise over this period (Figure 3), it is likely that other factors also contribute to the lack of change in the SO3 simulations.

The intensification of EKE becomes clear in both the AWI-CM-1 ensemble (Figure 1a), its members (Figure 3), and the SO3 simulations (Figure 1c) by the end of the 21st century. Over this period, the variability of EKE, indicated by the range of the distribution, also increases for each dataset (Figure 1f, i). EKE rise in SO3 is approximately three times that of the AWI-CM1 ensemble in absolute terms (Figure 1f), but expressing EKE as a relative value normalized by the mean and standard deviation of each dataset during the observational period (Figure 1g, h, i), reveals greater consistency between the changes until the end of the 21st century. EKE in each dataset appears to increase by approximately 3 standard deviations, and the range of EKE distributions increases by approximately one to two standard deviations (Figure 1h, i).

https://doi.org/10.5194/egusphere-2023-1496
Preprint. Discussion started: 14 July 2023

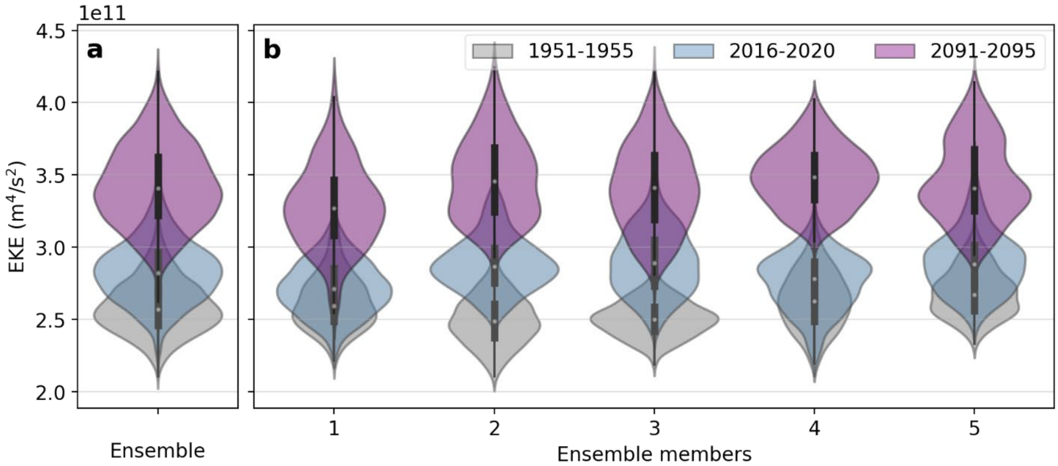

Figure 3. Ensemble spread of EKE in AWI-CM-1. a) Violin plots of mean Southern Ocean EKE in the AWI-CM-1 ensemble. **b)** Violin plots of mean Southern Ocean EKE in each member of the AWI-CM-1 ensemble. Grey plots represent the period 1951-1955, blue plots represent 2016-2020, purple plots represent 2091-2095.

Before considering the regional impacts of warming on EKE in the SO3 simulations, it is useful to refer to the ensemble spread within the AWI-CM-1 simulations to approximate the reliability of a single ensemble member in revealing the ensemble-mean change as an analogue to the signal-to-noise ratio. At 1 °C of warming, EKE change in the ensemble is weak, with at least one ensemble member tending to show little or no EKE change in most regions (Figure 4a,c). Only a few clear patterns of change emerge throughout the ensemble, namely the regions of EKE intensification downstream of the Kerguelen Plateau and the Campbell Plateau where four to five out of five ensemble members show clear EKE intensification (Figure 4a). It should be noted that even in these regions of relatively high confidence (4 to 5 ensemble members, Figure 4a) EKE rise can be interspersed with lower-confidence (1 to 2 ensemble members, Figure 4c) EKE decline; this is also illustrated by the ensemble mean changes themselves (Supplementary Figures 2, 3). Despite this, the consistency of EKE rise in these regions, and their geographic positions in already EKE-rich regions, suggests that the intensification patterns are

https://doi.org/10.5194/egusphere-2023-1496
Preprint. Discussion started: 14 July 2023

robust changes within substantial noise. This level of noise suggests that EKE changes in the SO3 simulations at 1 °C of warming will be difficult to distinguish from natural variability when taken on their own; indeed, in the SO3 simulations, the large variability of both sign and magnitude of change within relatively small spatial scales does not lend confidence to any significant change at 1 °C of warming (Figure 5c). However, building on the changes observed in the AWI-CM-1 ensemble, the intensification of EKE downstream of the Kerguelen and Campbell Plateaus seems to be reinforced by the high-resolution simulations.

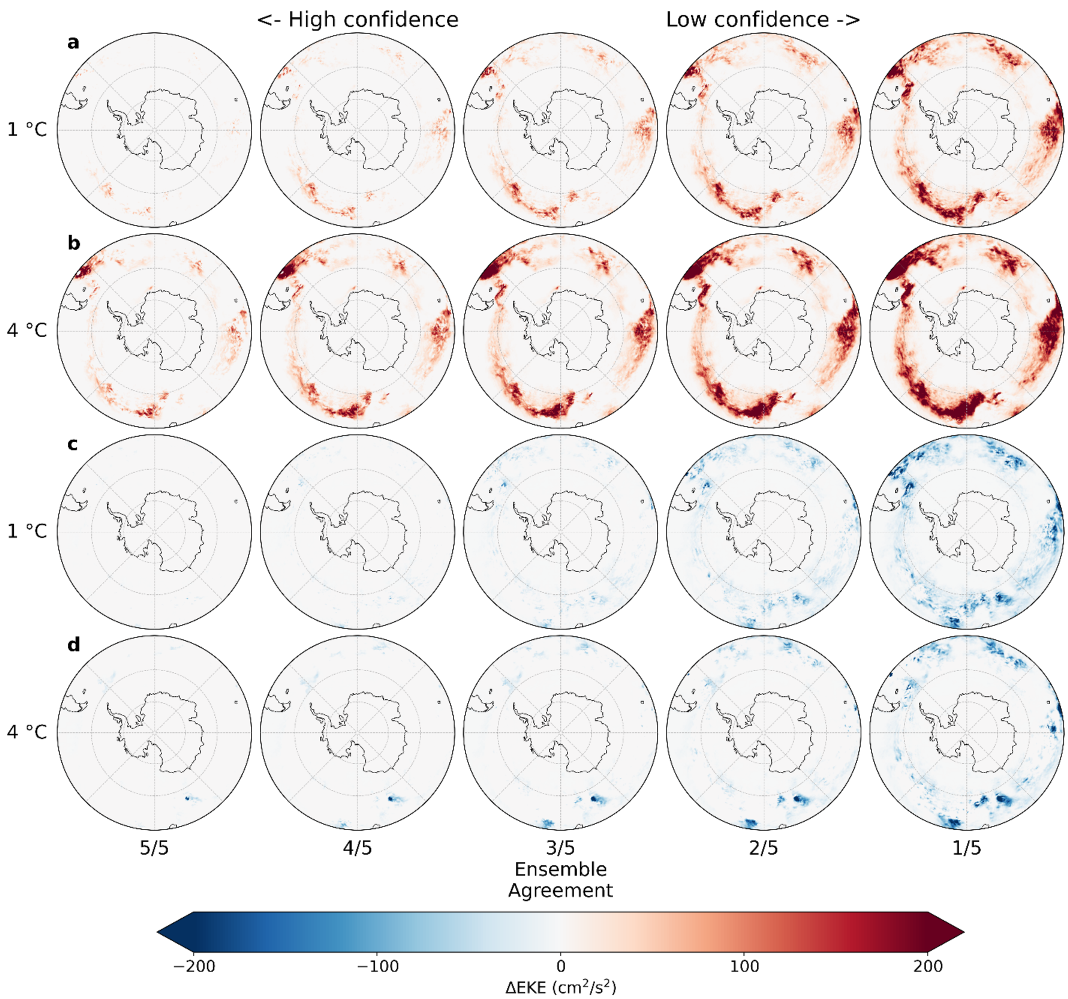

https://doi.org/10.5194/egusphere-2023-1496
Preprint. Discussion started: 14 July 2023

Figure 4. Ensemble agreement regarding EKE rise (a, b) and decline (c, d) within the AWI-CM-1 ensemble after one (a, c) and four (b, d) °C of warming. Ensemble agreement refers to the number of ensemble members that simulate at least the pictured magnitude of EKE rise or decline for each grid cell. Rank 5/5 indicates the lowest magnitude of EKE rise or decline within the ensemble for a given grid cell, meaning the entire ensemble agrees on at least this much change. Rank 1/5 indicates the highest magnitude of EKE rise or decline within the ensemble for each grid cell, representing the upper limit of projected EKE change.

At 4 °C of warming, change in eddy activity becomes clearer; EKE intensification downstream of the Kerguelen and Campbell Plateaus is now consistent throughout the entire AWI-CM-1 ensemble, along with additional intensifications south of the Falkland/Malvinas Plateau, around the Conrad Rise, and along the Antarctic Slope Current at approximately 5 °E (Figure 4b). Four fifths of the ensemble also include a broad increase in EKE throughout the ACC across most longitudes. Interestingly, a consistent pattern of EKE decline also emerges upstream of the Campbell Plateau in the entire ensemble (Figure 4d). The spatial pattern of EKE rise is relatively consistent regardless of confidence, with only the magnitude increasing in the lower confidence composites (Figure 4b). The same tendency is observable between the EKE changes at 1 and 4 °C of warming, where the magnitude of change is greater after further warming but follows the same spatial pattern. Thus, regions of intensification can be identified more reliably than the magnitude of change and tend to be concentrated where flow interacts with topographic features, in already eddy-rich regions (Figure 2). Conversely, low confidence EKE decline appears nearly throughout the Southern Ocean in at least one ensemble member, but only consistently upstream of the Campbell Plateau and, to a far lesser extent, downstream of the Drake Passage and Campbell Plateau (Figure 4d). Changes of negative sign tend to be of lower magnitude at 4 °C of warming than at 1 °C. This suggests that in any given single ensemble simulation, a robust general intensification of EKE tends to occur but can be interspersed with spurious signals of decline. Yet, small regions of high-confidence EKE decline are also possible, however uncommon. Consequently, it would be difficult to confidently separate reliable

https://doi.org/10.5194/egusphere-2023-1496
Preprint. Discussion started: 14 July 2023

EKE change from natural variability in simulations without an ensemble to compare with. In the SO3 simulations, EKE rise downstream of the Drake Passage and Kerguelen and Campbell Plateaus is substantial (Figure 5f). EKE rise is also projected south of the Falkland/Malvinas Plateau, around the Conrad Rise, and along the Antarctic Slope Current at approximately 5 °E, and a slight EKE decline appears upstream of the Campbell Plateau. All of this is comparable to the AWI-CM-1 ensemble, and the interspersed areas of EKE decline within these regions, for example, around the Conrad Rise, are not improbable based on the example set by AWI-CM-1 (Figure 4d). However, considering that some high-confidence EKE decline is present in the AWI-CM-1 ensemble, it is difficult to confidently dismiss regional EKE decline in the SO3 simulations as noise.

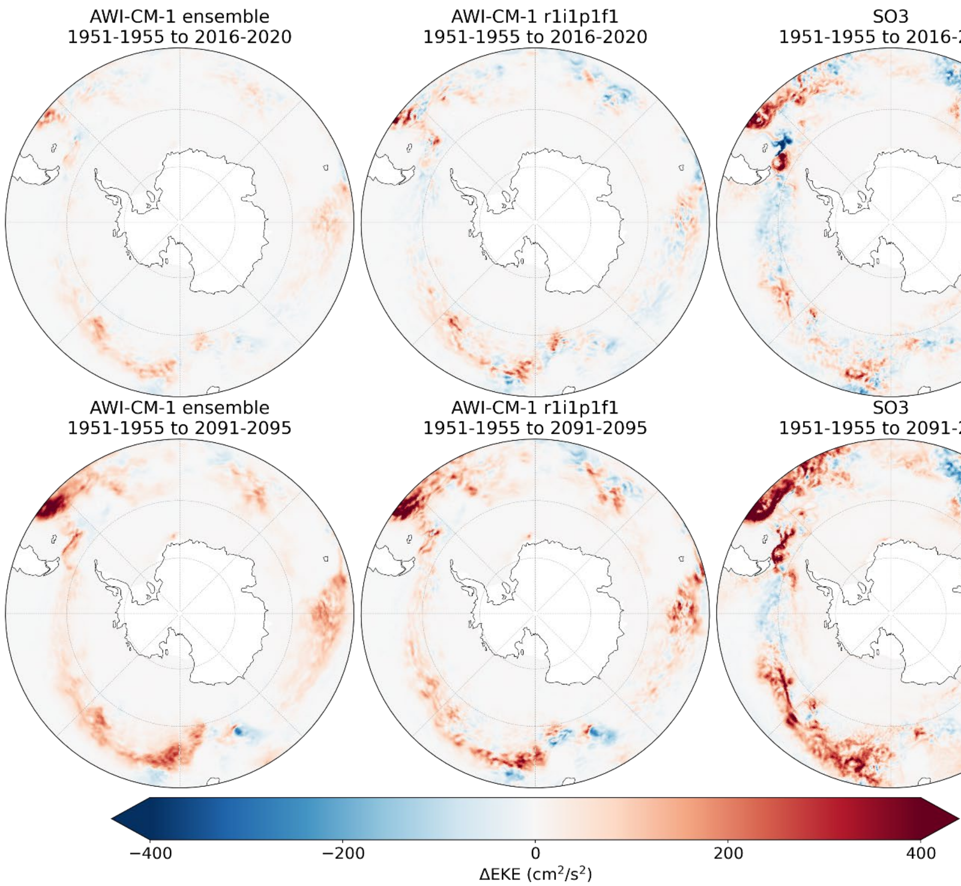

https://doi.org/10.5194/egusphere-2023-1496
Preprint. Discussion started: 14 July 2023

Figure 5. EKE change. Spatial representations of the difference in EKE between **(a-c)** 1951-1955 and 2016-2020, **(d-f)** 1951-1955 and 2091-2095. **a,d)** The AWI-CM-1 ensemble. **b,e)** the first member of the AWI-CM-1 ensemble. **c,f)** The SO3 simulations.

4 Discussion

Intensification of eddy activity in the Southern Ocean is now widely accepted as a consequence of anthropogenic climate change (Hogg et al., 2015; Patara et al., 2016; Martínez-Moreno et al., 2021; Beech et al., 2022), and Is understood to be caused primarily by stronger westerly winds imparting more energy to the Antarctic Circumpolar Current (Munday et al., 2013; Marshall, 2003). The results presented here reinforce the notion of EKE intensification and further project increased EKE variability as the climate warms (Figure 1, 3). Understanding of regional changes within the Southern Ocean eddy field is generally limited to regions defined by oceanic sectors (Atlantic, Indian, Pacific) (Hogg et al., 2015), or incremental longitudinal delimitations (Patara et al., 2016). By expressing EKE change in terms of ensemble agreement on a cell-by-cell basis, the results presented here are able to identify regions of reliable and substantial change as those where flow interacts with major bathymetric features, and high eddy activity is already known to occur (Figure 4). In future research, regional analyses of both the significance and cause of EKE trends could focus on these regions to avoid confounding results with those of physically unrelated change within the chosen geographic delimitations.

Considering the consistency of the AWI-CM-1 ensemble both in terms of representing mean EKE distribution (Supplementary Figure 2), and projecting overall Southern Ocean EKE change (Figure 2), it appears that a larger ensemble of high-resolution simulations is not necessary to assess local mean states and changes over the entire region. This also means that the discrepancies between the SO3 simulations and AWI-CM-1 ensemble remain unexplained. The SO3 simulations failed to reproduce the clear intensification of EKE present in the ensemble at 1 °C of warming, which has already been identified in observations (Martínez-Moreno et al., 2021). One potential explanation for this is the atmospheric forcing

https://doi.org/10.5194/egusphere-2023-1496
Preprint. Discussion started: 14 July 2023

applied to the SO3 simulations which cannot react to oceanic conditions in the same way that the real atmosphere or coupled atmosphere of the AWI-CM-1 ensemble can. Consequently, atmospheric forcing has been found to cause 27% more eddy killing by wind stress than coupled simulations (Renault et al., 2016). Since intensifying wind is widely considered the cause of EKE intensification in the Southern Ocean (Meredith and Hogg, 2006; Munday et al., 2013; Hogg et al., 2015; Beech et al., 2022), the increase may be counteracted by a simultaneous increase in eddy killing.

Assuming that the medium-resolution spin-up simulation effectively imparts a generally equilibrated ocean to the SO3 simulations in terms of baroclinic and barotropic instability, the remaining discrepancies between eddy activity in SO3 and observations should be largely identifiable. In terms of grid resolution, resolving the first Rossby radius of deformation with at least two grid points is not enough to comprehensively reproduce mesoscale activity (Hallberg, 2013; Sein et al., 2017), meaning grid refinement may need to be expanded to regions that impact eddy dynamics in the Southern Ocean. Other sources of bias may include ocean-atmosphere interactions which are absent or unrealistic within the uncoupled simulations (Byrne et al., 2016; Rai et al., 2021; Renault et al., 2016). As well, some small-scale, slow-to-equilibrate ocean processes may be resolved in the high-resolution simulations, but not be integrated long enough for their effects to impact eddy activity (van Westen and Dijkstra, 2021; Rackow et al., 2022). Finally, the gridded altimetry product itself may be responsible for some disagreement, as the along-track data is known to underrepresent eddy activity at scales less than 150km and 10 days (Chassignet and Xu, 2017), which will be particularly impactful at high latitudes.

To distinguish a meaningful signal of anthropogenic impacts from natural variability, this analysis relies primarily on consistency among ensemble members (Figures 3, 4). This is distinct from more traditional methods like assessment of error relative to observations or ensemble mean, commonly applied to weather forecasting (Ferro et al., 2012). Performance evaluation relative to observations would undoubtedly point to the high-resolution simulation as superior due to the drastic underrepresentation of EKE in the eddy-permitting ensemble (Figure 1). Yet, the effects of climate change are still apparent in

https://doi.org/10.5194/egusphere-2023-1496
Preprint. Discussion started: 14 July 2023

the AWI-CM-1 ensemble (Figure 1, 5), and the AWI-CM-1 dataset has been used to make similar projections of EKE already (Beech et al., 2022). Moreover, the eddy response to forcing seems to be consistent between the model resolutions when expressed in relative (Figure 1g, h, i), rather than absolute terms (Figure 1a, b, c). While more verification of this result is necessary both regionally, and with other models, these results suggest that eddy-permitting resolutions can be interpreted with their shortcomings in mind in order to discern the real-world implications: as is often necessary with model data. Thus, based on the test case of the Southern Ocean, the usefulness of the AWI-CM-1 ensemble and the effectiveness of model simulations in identifying physically significant and reproduceable impacts of climate change may be greater than would be identified using traditional methods and comes at a much lower cost relative to the eddy-resolving simulations.

This study has focused on EKE as an evaluation metric for the simulations since mesoscale activity is the primary motivation for increasing ocean model resolution. It has stopped short of assessing the improvements that resolving the mesoscale has on climate and ocean dynamics, many of which are discussed in detail elsewhere (eg. (Hewitt et al., 2017). Rather than repeat an assessment of the benefits of resolving smaller scales, we assume that the accurate reproduction and evolution of eddy activity indicates that these improvements are transferred to broader processes. Certainly, inaccurate simulation of the mesoscale would raise questions regarding the improvements that this mesoscale activity should have on the simulations as a whole. Nonetheless, further evaluation of the modeling approaches employed in this study will be necessary to determine if these methods are appropriate for studying broader elements of the climate system. Since the high-resolution simulations derive their deep-ocean climate primarily from the medium-resolution spin-up simulation, improving the initialization process (Thiria et al., 2023) may be the critical barrier to extending these results from the mixed layer to the deeper ocean.

5 Conclusion

Resolving the ocean mesoscale has become a focus for the climate and ocean modeling community as computational capabilities expand and models become increasingly complex. The benefits that explicitly resolved eddy activity can have on climate simulations are clear (Hewitt et al., 2017; Sein et al., 2017) along with the impact that mesoscale variability has on local (Lachkar et al., 2009; Wang et al., 2017) and global environments (Falkowski et al., 1991; Sallée et al., 2012). However, state-of-the-art climate models will be unable to fully resolve the mesoscale for the foreseeable future, particularly in large-scale modeling endeavors such as CMIP (Hewitt et al., 2020). Thus, modelers must make informed choices regarding the explicit processes needed to answer research questions and where resources must be allocated to achieve specific goals. Existing analysis of resource allocation has typically addressed short-term weather forecasting or the ability to reproduce observations with low error (Ferro et al., 2012), but the question of how to best allocate resources for climate change impact assessment remains. This study has applied several cost-efficient modeling approaches to an analysis of the impacts of climate change on a key focus of high-resolution modeling: the mesoscale. Applying these results to broader climate change impact studies should improve the efficiency of resource allocation and focus modeling studies. Resolution can be dynamically adjusted both spatially, by focusing resources in study regions and where they are necessary to resolve local dynamics, and temporally, by allowing lower-resolution workhorse configurations to perform spin-up and transient runs. Limited simulation length and ensemble size can be sufficient for certain research questions and validation, but simulations must ultimately be designed to meet their specific goals. Where resources are limited, studies may best include a combination of eddy-resolving simulations able to fully capture the local eddy field, as well as eddy-present simulations that can attest to the significance of results through consistency and repetition.

This work represents a contribution to the growing wealth of research that points to an intensification of eddy activity in the Southern Ocean (Hogg et al., 2015; Martínez-Moreno et al., 2021; Beech et al., 2022). The further conclusions that EKE variability may increase and that EKE intensification appears concentrated in key regions based on topography can both expand the present state of knowledge, as well as direct future research. The cost-efficient modelling approaches of regional grid refinement, reduced-resolution spin-up and transient runs, and limited simulation lengths distinguished by

https://doi.org/10.5194/egusphere-2023-1496
Preprint. Discussion started: 14 July 2023

longer periods of change are demonstrated to be effective at reproducing change within a more traditional eddy-permitting ensemble. When resources are limited and resolution demands are high, these approaches can be adapted to address specific research questions. Where assessing the robustness of change is critical, the complimentary eddy-permitting ensemble represents an effective, low-cost supplement to the high-resolution simulations.

Data Availability

Geostrophic velocities derived from satellite altimetry data are publicly available at https://doi.org/10.48670/moi-00148. Daily sea surface height data from AWI-CM-1-1-MR in CMIP6 used to compute geostrophic velocities in this study is archived at the World Data Center for Climate at the DKRZ (https://doi.org/10.26050/WDCC/C6sCMAWAWM, https://doi.org/10.26050/WDCC/C6sSPAWAWM) (Semmler et al., 2022a, b). Model output from AWI-CM-1-1-MR in the CMIP6 framework, including all variables used to force the standalone ocean simulations conducted for this study, is publicly available at https://doi.org/10.22033/ESGF/CMIP6.359 (Semmler et al., 2018). Eddy kinetic energy datasets calculated from FESOM output velocities are available at (https://doi.org/10.5281/zenodo.8046792) (Beech, 2023b).

Code Availability

Source code for the ocean model FESOM version 2.5 is available at (https://doi.org/10.5281/zenodo.7737061) (patrickscholz et al., 2023). Code used for data analysis and visualization in this study is publicly available at (https://doi.org/10.5281/zenodo.8046783) (Beech, 2023a). Code used to calculate geostrophic velocities from sea surface height data from AWI-CM-1-1-MR is available from https://doi.org/10.5281/zenodo.7050573.

Author Contributions

NB, TJ, TR, and TS conceived of the study. NB carried out the simulations, analyzed the data, and drafted the manuscript. All authors reviewed the manuscript.

Competing Interests

The authors declare no competing interests.

Acknowledgements

https://doi.org/10.5194/egusphere-2023-1496
Preprint. Discussion started: 14 July 2023

The work described in this paper has received funding from the Helmholtz Association through the project 'Advanced Earth System Model Capacity' (project leader: T.J., support code: ZT-0003) in the frame of the initiative 'Zukunftsthemen'. The content of the paper is the sole responsibility of the authors and it does not represent the opinion of the Helmholtz Association, and the Helmholtz Association is not responsible for any use that might be made of information contained. TJ acknowledges the EERIE project funded under the EU Horizon Europe programme (grant number 101081383). TR acknowledges support from the European Commission's Horizon 2020 collaborative project NextGEMS (grant number 101003470). This work used resources of the Deutsches Klimarechenzentrum (DKRZ) granted by its Scientific Steering Committee (WLA) under project ID 995. The CMIP data used in this study were replicated and made available by the DKRZ.

https://doi.org/10.5194/egusphere-2023-1496
Preprint. Discussion started: 14 July 2023

References

Auger, M., Prandi, P., and Sallée, J.-B.: Southern ocean sea level anomaly in the sea ice-covered sector from multimission satellite observations, Sci. Data, 9, 70, https://doi.org/10.1038/s41597-022-01166-z, 2022.

Auger, M., Sallée, J.-B., Thompson, A. F., Pauthenet, E., and Prandi, P.: Southern Ocean Ice-Covered Eddy Properties From Satellite Altimetry, J. Geophys. Res. Oceans, 128, e2022JC019363, https://doi.org/10.1029/2022JC019363, 2023.

Ballarotta, M., Ubelmann, C., Pujol, M.-I., Taburet, G., Fournier, F., Legeais, J.-F., Faugère, Y., Delepoulle, A., Chelton, D., Dibarboure, G., and Picot, N.: On the resolutions of ocean altimetry maps, Ocean Sci., 15, 1091–1109, https://doi.org/10.5194/os-15-1091-2019, 2019.

Beech, N.: n-beech/SO_meso: Initial release, https://doi.org/10.5281/zenodo.8046783, 2023a.

Beech, N.: Processed EKE from FESOM-SO3 (1.0), https://doi.org/10.5281/zenodo.8046792, 2023b.

Beech, N., Rackow, T., Semmler, T., Danilov, S., Wang, Q., and Jung, T.: Long-term evolution of ocean eddy activity in a warming world, Nat. Clim. Change, 12, 910–917, https://doi.org/10.1038/s41558-022-01478-3, 2022.

Bishop, S. P., Gent, P. R., Bryan, F. O., Thompson, A. F., Long, M. C., and Abernathey, R.: Southern Ocean Overturning Compensation in an Eddy-Resolving Climate Simulation, J. Phys. Oceanogr., 46, 1575–1592, https://doi.org/10.1175/JPO-D-15-0177.1, 2016.

Bronselaer, B., Winton, M., Griffies, S. M., Hurlin, W. J., Rodgers, K. B., Sergienko, O. V., Stouffer, R. J., and Russell, J. L.: Change in future climate due to Antarctic meltwater, Nature, 564, 53–58, https://doi.org/10.1038/s41586-018-0712-z, 2018.

Byrne, D., Münnich, M., Frenger, I., and Gruber, N.: Mesoscale atmosphere ocean coupling enhances the transfer of wind energy into the ocean, Nat. Commun., 7, ncomms11867, https://doi.org/10.1038/ncomms11867, 2016.

Chassignet, E. P. and Xu, X.: Impact of Horizontal Resolution (1/12° to 1/50°) on Gulf Stream Separation, Penetration, and Variability, J. Phys. Oceanogr., 47, 1999–2021, https://doi.org/10.1175/JPO-D-17-0031.1, 2017.

Danilov, S.: Ocean modeling on unstructured meshes, Ocean Model., 69, 195–210, https://doi.org/10.1016/j.ocemod.2013.05.005, 2013.

Danilov, S., Sidorenko, D., Wang, Q., and Jung, T.: The Finite-volumE Sea ice–Ocean Model (FESOM2), Geosci. Model Dev., 10, 765–789, https://doi.org/10.5194/gmd-10-765-2017, 2017.

Eyring, V., Bony, S., Meehl, G. A., Senior, C. A., Stevens, B., Stouffer, R. J., and Taylor, K. E.: Overview of the Coupled Model Intercomparison Project Phase 6 (CMIP6) experimental design and organization, Geosci. Model Dev., 9, 1937–1958, https://doi.org/10.5194/gmd-9-1937-2016, 2016.

Falkowski, P. G., Ziemann, D., Kolber, Z., and Bienfang, P. K.: Role of eddy pumping in enhancing primary production in the ocean, Nature, 352, 55–58, https://doi.org/10.1038/352055a0, 1991.

https://doi.org/10.5194/egusphere-2023-1496
Preprint. Discussion started: 14 July 2023

Ferrari, R., Griffies, S. M., Nurser, A. J. G., and Vallis, G. K.: A boundary-value problem for the parameterized mesoscale eddy transport, Ocean Model., 32, 143–156, https://doi.org/10.1016/j.ocemod.2010.01.004, 2010.

Ferro, C. A. T., Jupp, T. E., Lambert, F. H., Huntingford, C., and Cox, P. M.: Model complexity versus ensemble size: allocating resources for climate prediction, Philos. Trans. R. Soc. Math. Phys. Eng. Sci., 370, 1087–1099, https://doi.org/10.1098/rsta.2011.0307, 2012.

Frölicher, T. L., Sarmiento, J. L., Paynter, D. J., Dunne, J. P., Krasting, J. P., and Winton, M.: Dominance of the Southern Ocean in Anthropogenic Carbon and Heat Uptake in CMIP5 Models, J. Clim., 28, 862–886, https://doi.org/10.1175/JCLI-D-14-00117.1, 2015.

Gent, P. R. and McWilliams, J. C.: Isopycnal Mixing in Ocean Circulation Models, J. Phys. Oceanogr., 20, 150–155, https://doi.org/10.1175/1520-0485(1990)020<0150:IMIOCM>2.0.CO;2, 1990.

Haarsma, R. J., Roberts, M. J., Vidale, P. L., Senior, C. A., Bellucci, A., Bao, Q., Chang, P., Corti, S., Fučkar, N. S., Guemas, V., von Hardenberg, J., Hazeleger, W., Kodama, C., Koenigk, T., Leung, L. R., Lu, J., Luo, J.-J., Mao, J., Mizielinski, M. S., Mizuta, R., Nobre, P., Satoh, M., Scoccimarro, E., Semmler, T., Small, J., and von Storch, J.-S.: High Resolution Model Intercomparison Project (HighResMIP v1.0) for CMIP6, Geosci. Model Dev., 9, 4185–4208, https://doi.org/10.5194/gmd-9-4185-2016, 2016.

Hallberg, R.: Using a resolution function to regulate parameterizations of oceanic mesoscale eddy effects, Ocean Model., 72, 92–103, https://doi.org/10.1016/j.ocemod.2013.08.007, 2013.

Hewitt, H. T., Bell, M. J., Chassignet, E. P., Czaja, A., Ferreira, D., Griffies, S. M., Hyder, P., McClean, J. L., New, A. L., and Roberts, M. J.: Will high-resolution global ocean models benefit coupled predictions on short-range to climate timescales?, Ocean Model., 120, 120–136, https://doi.org/10.1016/j.ocemod.2017.11.002, 2017.

Hewitt, H. T., Roberts, M., Mathiot, P., Biastoch, A., Blockley, E., Chassignet, E. P., Fox-Kemper, B., Hyder, P., Marshall, D. P., Popova, E., Treguier, A.-M., Zanna, L., Yool, A., Yu, Y., Beadling, R., Bell, M., Kuhlbrodt, T., Arsouze, T., Bellucci, A., Castruccio, F., Gan, B., Putrasahan, D., Roberts, C. D., Van Roekel, L., and Zhang, Q.: Resolving and Parameterising the Ocean Mesoscale in Earth System Models, Curr. Clim. Change Rep., 6, 137–152, https://doi.org/10.1007/s40641-020-00164-w, 2020.

Hogg, A. McC., Meredith, M. P., Chambers, D. P., Abrahamsen, E. P., Hughes, C. W., and Morrison, A. K.: Recent trends in the Southern Ocean eddy field, J. Geophys. Res. Oceans, 120, 257–267, https://doi.org/10.1002/2014JC010470, 2015.

Irving, D., Hobbs, W., Church, J., and Zika, J.: A Mass and Energy Conservation Analysis of Drift in the CMIP6 Ensemble, J. Clim., 34, 3157–3170, https://doi.org/10.1175/JCLI-D-20-0281.1, 2021.

Jungclaus, J. H., Lorenz, S. J., Schmidt, H., Brovkin, V., Brüggemann, N., Chegini, F., Crüger, T., De-Vrese, P., Gayler, V., Giorgetta, M. A., Gutjahr, O., Haak, H., Hagemann, S., Hanke, M., Ilyina, T., Korn, P., Kröger, J., Linardakis, L., Mehlmann, C., Mikolajewicz, U., Müller, W. A., Nabel, J. E. M. S., Notz, D., Pohlmann, H., Putrasahan, D. A., Raddatz, T., Ramme, L., Redler, R., Reick, C. H., Riddick, T., Sam, T., Schneck, R., Schnur, R., Schupfner, M., von Storch, J.-S., Wachsmann, F., Wieners, K.-H., Ziemen, F., Stevens, B., Marotzke, J., and Claussen, M.: The ICON Earth System Model Version 1.0, J. Adv. Model. Earth Syst., 14, e2021MS002813, https://doi.org/10.1029/2021MS002813, 2022.

Lachkar, Z., Orr, J. C., Dutay, J. C., and Delecluse, P.: On the role of mesoscale eddies in the ventilation of Antarctic intermediate water, Deep-Sea Res. Part Oceanogr. Res. Pap., 56, 909–925, https://doi.org/10.1016/j.dsr.2009.01.013, 2009.

Landschützer, P., Gruber, N., Haumann, F. A., Rödenbeck, C., Bakker, D. C. E., van Heuven, S., Hoppema, M., Metzl, N., Sweeney, C., Takahashi, T., Tilbrook, B., and Wanninkhof, R.: The reinvigoration of the Southern Ocean carbon sink, Science, 349, 1221–1224, https://doi.org/10.1126/science.aab2620, 2015.

Large, W. G., McWilliams, J. C., and Doney, S. C.: Oceanic vertical mixing: A review and a model with a nonlocal boundary layer parameterization, Rev. Geophys., 32, 363–403, https://doi.org/10.1029/94RG01872, 1994.

Marshall, G. J.: Trends in the Southern Annular Mode from Observations and Reanalyses, J. Clim., 16, 4134–4143, https://doi.org/10.1175/1520-0442(2003)016<4134:TITSAM>2.0.CO;2, 2003.

Martínez-Moreno, J., Hogg, A. McC., England, M. H., Constantinou, N. C., Kiss, A. E., and Morrison, A. K.: Global changes in oceanic mesoscale currents over the satellite altimetry record, Nat. Clim. Change, 11, 397–403, https://doi.org/10.1038/s41558-021-01006-9, 2021.

Marzocchi, A., Hirschi, J. J.-M., Holliday, N. P., Cunningham, S. A., Blaker, A. T., and Coward, A. C.: The North Atlantic subpolar circulation in an eddy-resolving global ocean model, J. Mar. Syst., 142, 126–143, https://doi.org/10.1016/j.jmarsys.2014.10.007, 2015.

Meredith, M. P. and Hogg, A. M.: Circumpolar response of Southern Ocean eddy activity to a change in the Southern Annular Mode, Geophys. Res. Lett., 33, https://doi.org/10.1029/2006GL026499, 2006.

Munday, D. R., Johnson, H. L., and Marshall, D. P.: Eddy Saturation of Equilibrated Circumpolar Currents, J. Phys. Oceanogr., 43, 507–532, https://doi.org/10.1175/JPO-D-12-095.1, 2013.

O'Neill, B. C., Tebaldi, C., van Vuuren, D. P., Eyring, V., Friedlingstein, P., Hurtt, G., Knutti, R., Kriegler, E., Lamarque, J.-F., Lowe, J., Meehl, G. A., Moss, R., Riahi, K., and Sanderson, B. M.: The Scenario Model Intercomparison Project (ScenarioMIP) for CMIP6, Geosci. Model Dev., 9, 3461–3482, https://doi.org/10.5194/gmd-9-3461-2016, 2016.

O'Neill, B. C., Kriegler, E., Ebi, K. L., Kemp-Benedict, E., Riahi, K., Rothman, D. S., van Ruijven, B. J., van Vuuren, D. P., Birkmann, J., Kok, K., Levy, M., and Solecki, W.: The roads ahead: Narratives for shared socioeconomic pathways describing world futures in the 21st century, Glob. Environ. Change, 42, 169–180, https://doi.org/10.1016/j.gloenvcha.2015.01.004, 2017.

Patara, L., Böning, C. W., and Biastoch, A.: Variability and trends in Southern Ocean eddy activity in 1/12° ocean model simulations, Geophys. Res. Lett., 43, 4517–4523, https://doi.org/10.1002/2016GL069026, 2016.

patrickscholz, dsidoren, Koldunov, N., Hegewald, J., rakowsk, Streffing, J., Rackow, T., ogurses, helgegoessling, Guibert, D., qiangclimate, cwekerle, Oord, G. van den, jrberlin, Miguel, Gierz, P., and Cheedela, S. K.: FESOM/fesom2: FESOM2.5, , https://doi.org/10.5281/zenodo.7737061, 2023.

https://doi.org/10.5194/egusphere-2023-1496
Preprint. Discussion started: 14 July 2023

Pauling, A. G., Smith, I. J., Langhorne, P. J., and Bitz, C. M.: Time-Dependent Freshwater Input From Ice Shelves: Impacts on Antarctic Sea Ice and the Southern Ocean in an Earth System Model, Geophys. Res. Lett., 44, 10,454-10,461, https://doi.org/10.1002/2017GL075017, 2017.

Rackow, T., Danilov, S., Goessling, H. F., Hellmer, H. H., Sein, D. V., Semmler, T., Sidorenko, D., and Jung, T.: Delayed Antarctic sea-ice decline in high-resolution climate change simulations, Nat. Commun., 13, 637, https://doi.org/10.1038/s41467-022-28259-y, 2022.

Rai, S., Hecht, M., Maltrud, M., and Aluie, H.: Scale of oceanic eddy killing by wind from global satellite observations, Sci. Adv., 7, eabf4920, https://doi.org/10.1126/sciadv.abf4920, 2021.

Renault, L., Molemaker, M. J., McWilliams, J. C., Shchepetkin, A. F., Lemarié, F., Chelton, D., Illig, S., and Hall, A.: Modulation of Wind Work by Oceanic Current Interaction with the Atmosphere, J. Phys. Oceanogr., 46, 1685–1704, https://doi.org/10.1175/JPO-D-15-0232.1, 2016.

Ringler, T., Petersen, M., Higdon, R. L., Jacobsen, D., Jones, P. W., and Maltrud, M.: A multi-resolution approach to global ocean modeling, Ocean Model., 69, 211–232, https://doi.org/10.1016/j.ocemod.2013.04.010, 2013.

Sallée, J.-B., Matear, R. J., Rintoul, S. R., and Lenton, A.: Localized subduction of anthropogenic carbon dioxide in the Southern Hemisphere oceans, Nat. Geosci., 5, 579–584, https://doi.org/10.1038/ngeo1523, 2012.

Scholz, P., Sidorenko, D., Gurses, O., Danilov, S., Koldunov, N., Wang, Q., Sein, D., Smolentseva, M., Rakowsky, N., and Jung, T.: Assessment of the Finite-volumE Sea ice-Ocean Model (FESOM2.0) – Part 1: Description of selected key model elements and comparison to its predecessor version, Geosci. Model Dev., 12, 4875–4899, https://doi.org/10.5194/gmd-12-4875-2019, 2019.

Scholz, P., Sidorenko, D., Danilov, S., Wang, Q., Koldunov, N., Sein, D., and Jung, T.: Assessment of the Finite VolumE Sea Ice Ocean Model (FESOM2.0), Part II: Partial bottom cells, embedded sea ice and vertical mixing library CVMIX, Climate and Earth system modeling, https://doi.org/10.5194/gmd-2021-94, 2021.

Sein, D. V., Koldunov, N. V., Danilov, S., Wang, Q., Sidorenko, D., Fast, I., Rackow, T., Cabos, W., and Jung, T.: Ocean Modeling on a Mesh With Resolution Following the Local Rossby Radius, J. Adv. Model. Earth Syst., 9, 2601–2614, https://doi.org/10.1002/2017MS001099, 2017.

Semmler, T., Danilov, S., Rackow, T., Sidorenko, D., Barbi, D., Hegewald, J., Sein, D., Wang, Q., and Jung, T.: AWI AWI-CM1.1MR model output prepared for CMIP6 CMIP, https://doi.org/10.22033/ESGF/CMIP6.359, 2018.

Semmler, T., Danilov, S., Gierz, P., Goessling, H. F., Hegewald, J., Hinrichs, C., Koldunov, N., Khosravi, N., Mu, L., Rackow, T., Sein, D. V., Sidorenko, D., Wang, Q., and Jung, T.: Simulations for CMIP6 With the AWI Climate Model AWI-CM-1-1, J. Adv. Model. Earth Syst., 12, e2019MS002009, https://doi.org/10.1029/2019MS002009, 2020.

Semmler, T., Danilov, S., Rackow, T., Sidorenko, D., Barbi, D., Hegewald, J., Sein, D., Wang, Q., and Jung, T.: CMIP6_supplemental CMIP AWI AWI-CM-1-1-MR, https://doi.org/10.26050/WDCC/C6sCMAWAWM, 2022a.

https://doi.org/10.5194/egusphere-2023-1496
Preprint. Discussion started: 14 July 2023

Semmler, T., Danilov, S., Rackow, T., Sidorenko, D., Barbi, D., Hegewald, J., Sein, D., Wang, Q., and Jung, T.: CMIP6_supplemental ScenarioMIP AWI AWI-CM-1-1-MR, https://doi.org/10.26050/WDCC/C6sSPAWAWM, 2022b.

Taburet, G., Sanchez-Roman, A., Ballarotta, M., Pujol, M.-I., Legeais, J.-F., Fournier, F., Faugere, Y., and Dibarboure, G.: DUACS DT2018: 25 years of reprocessed sea level altimetry products, Ocean Sci., 15, 1207–1224, https://doi.org/10.5194/os-15-1207-2019, 2019.

Thiria, S., Sorror, C., Archambault, T., Charantonis, A., Bereziat, D., Mejia, C., Molines, J.-M., and Crépon, M.: Downscaling of ocean fields by fusion of heterogeneous observations using Deep Learning algorithms, Ocean Model., 182, 102174, https://doi.org/10.1016/j.ocemod.2023.102174, 2023.

Wang, Q., Danilov, S., Sidorenko, D., Timmermann, R., Wekerle, C., Wang, X., Jung, T., and Schröter, J.: The Finite Element Sea Ice-Ocean Model (FESOM) v.1.4: formulation of an ocean general circulation model, Geosci. Model Dev., 7, 663–693, https://doi.org/10.5194/gmd-7-663-2014, 2014.

Wang, Y., Claus, M., Greatbatch, R. J., and Sheng, J.: Decomposition of the Mean Barotropic Transport in a High-Resolution Model of the North Atlantic Ocean, Geophys. Res. Lett., 44, 11,537-11,546, https://doi.org/10.1002/2017GL074825, 2017.

van Westen, R. M. and Dijkstra, H. A.: Ocean eddies strongly affect global mean sea-level projections, Sci. Adv., 7, eabf1674, https://doi.org/10.1126/sciadv.abf1674, 2021.

Yu, X., Ponte, A. L., Lahaye, N., Caspar-Cohen, Z., and Menemenlis, D.: Geostrophy Assessment and Momentum Balance of the Global Oceans in a Tide- and Eddy-Resolving Model, J. Geophys. Res. Oceans, 126, e2021JC017422, https://doi.org/10.1029/2021JC017422, 2021.